

An Optical Model of Tone Reproduction in Hard Copy Halftones

J. S. Arney

Center for Imaging Science, Rochester Institute of Technology

Rochester, New York

P. G. Engeldrum

Imcotek, Inc., Winchester, Massachusetts

Abstract

Pictorial tone reproduction with most non-impact printing technologies requires some sort of halftoning process, and the literature on digital halftoning is growing rapidly. However, an understanding of the halftoning algorithm is not sufficient to predict and understand tone reproduction. Physical and optical interactions between the colorant and the substrate are also essential elements of tone reproduction, and these factors become more and more dominant in governing tonal characteristics as the spatial addressability of print engines increases. This report describes a theoretical basis for a recently published model of the optical factors governing tone reproduction in halftone images. The theory is based the Fourier description of a one dimensional halftone and is supported by experimental data from one dimensional, line type halftones printed on paper. The model, based on the Murray-Davies equation, rationalizes non-linear effects without resorting to the Yule-Nielsen equation.

Introduction

Recent advances in the development of algorithms for digital halftoning have lead to significant improvements in the ability of non-impact printers to produce excellent pictorial tone while minimizing undesirable noise patterns.¹ However, the quality of pictorial tone reproduction depends as much on the physical and optical properties of colorants and substrates as on the algorithm which produces the halftone pattern. These optical and physical effects are well known in traditional printing technology and are often referred to as “dot gain”. For example, if a print engine is instructed to print a 50% dot (dot fraction $F_i = 0.5$), then one would expect a mean reflectance, R , half way between the unprinted paper, R_p , and the 100% dot, R_i . This linear relationship between F_i and R is described by the “Murray-Davies” equation.² However, the relationship between F_i and R is typically found

$$R = F_i R_i + (1 - F_i) R_p \quad (1)$$

to be non-linear, and measured reflectance factors are lower than predicted by equation (1).

There are two reasons for the non-linearity between F_i and R . First, the print engine may cause the colorant to spread out physically to produce a halftone dot that is larger than intended. Such physical “dot gain” effects are specific to each printing technology and will not be discussed here. The second cause of non-linearity, however, is an optical effect that is universal to all colorant-on-paper halftones. Light which strikes the paper between halftone dots is scattered laterally, and this lateral scatter increases the probability of light absorption by the halftone dot. The dot, therefore, has an effective absorption cross section that is larger than the physical cross section. The result is an optical “dot gain” and a non-linear relationship between F_i and R .

$$R(F_i) = [F_i R_i^{1/n} + (1 - F_i) R_p^{1/n}]^n \quad (2)$$

The Yule-Nielsen equation has been used successfully for several decades as an empirical model of halftone imaging³. The empirical “ n ” factor is adjusted to fit the non-linear relationship between F_i and R . While equation (2) often provides an adequate empirical model for halftone imaging, the apparent non-linear addition of photon flux implied by equation (2) is contrary to physical expectation, and the n power factor is not easily estimated from fundamental optical parameters characteristic of the colorant and paper.

$$R_p(F_p) = R_g [1 - (1 - T_i)(1 - F_p^w)] \cdot [1 - (1 - T_i)(1 - F_p^v)] \quad (3)$$

$$R_i(F_i) = R_g [1 - (1 - T_i)F_i^w] \cdot [1 - (1 - T_i)F_i^v] \quad (4)$$

Recent studies of the microstructure of halftone images produced by a variety of impact and non-impact technologies has shown the non-linearity between R and F_i occurs because R_i and R_p are themselves functions of the dot area, F_i .^{4,5} An empirical model, represented by equations (3) and (4), was developed and shown to fit well with image microstructure data from a variety of halftone types ranging from stochastic to clustered dot⁴. In these equations, R_g is the reflectance of the unprinted paper, T_i is the transmittance of the ink layer at $F_i = 1$, and $F_p = 1 - F_i$. The power terms, w and v , are identical in both equations and are adjusted empirically to achieve the least RMS difference between the equations and measured values of

paper and ink reflectances, R_p and R_i . The resulting values or R_p and R_i , when applied to equation (1), model R versus F_i as well as the Yule-Nielsen equation.⁴

A Fourier Description of One Dimensional Halftones

$$f_i(x) = F_p + \frac{2}{\pi} \sum_{n=1}^{\infty} \frac{-1^n}{n} \text{Sin}(n\pi F_p) \text{Cos}(2\pi n\omega_o x) \text{MTF}_i(n\omega_o) \quad (5)$$

$$T_i(x) = f_i(x)(1 - T_i) + T_i \quad (6)$$

The empirical arguments⁴ which lead to equations (3) and (4) suggested the power factor, w , is associated physically with the optical spread function, or MTF characteristic, of the paper. In addition, the power factor, v , is associated with the lateral distribution of colorant in the halftone dot. Based on a Fourier series description of a one dimensional halftone, these associations can be justified a priori. We begin with a description of the distribution of transmittance, T_i , in the halftone ink image. In one dimension, a square wave periodic function, $f_i(x)$, of spatial frequency ω_o , can be written as equation (5). The MTF term is inserted in order to describe the lateral distribution of the colorant. The transmittance pattern of the colorant is then given by equation (6). This is also the function which describes the irradiance pattern which enters the paper after passing the halftone dots.

After entering the paper, the photons are scattered. This is described by an MTF_p function characteristic of the paper. The photons are also absorbed, and this is described by the reflectance, R_g , of the unprinted paper. The overall photon flux which reflects back from the paper, but before re-encountering the dots, is described by equations (7) and (8).

$$I_r(x) = R_g [f_p(x)(1 - T_i) + T_i] \quad (7)$$

$$f_p(x) = F_p + \frac{2}{\pi} \sum_{n=1}^{\infty} \frac{-1^n}{n} \text{Sin}(n\pi F_p) \text{Cos}(2\pi n\omega_o x) \text{MTF}_i(n\omega_o) \text{MTF}_p(n\omega_o) \quad (8)$$

The spatial distribution of reflected light from the halftone is given by the product of equation (6) and (7). In addition, by averaging the fourier series over the range $x = F_i / 2\omega$ to $x = (2 - F_i) / 2\omega$, which is the range of x for the paper between the halftone dots, it can be shown that the mean reflectance of the paper between the dots is given by equation (9),

$$R_p(F_p) = R_g [G_p(F_p)(1 - T_i) + T_i] \cdot [G_i(F_p)(1 - T_i) + T_i] \quad (9)$$

where the Fourier series of equation (8) averages to the following functions of F_p ,

$$G_p(F_p) = F_p \sum_{n=-\infty}^{\infty} \text{Sinc}^2(nF_p) \text{MTF}_i(n\omega_o) \text{MTF}_p(n\omega_o) \quad (10)$$

$$G_i(F_p) = F_p \sum_{n=-\infty}^{\infty} \text{Sinc}^2(nF_p) \text{MTF}_i(n\omega_o) \quad (11)$$

Similar expressions can also be derived for the mean value of the reflectance of the halftone dots.

$$R_i(F_i) = R_g [H_p(F_i)(1 - T_i) + T_i] \cdot [H_i(F_i)(1 - T_i) + T_i] \quad (12)$$

$$H_p(F_i) = 1 - F_i \sum_{n=-\infty}^{\infty} \text{Sinc}^2(nF_i) \text{MTF}_i(n\omega_o) \text{MTF}_p(n\omega_o) \quad (13)$$

$$H_i(F_i) = 1 - F_i \sum_{n=-\infty}^{\infty} \text{Sinc}^2(nF_i) \text{MTF}_i(n\omega_o) \quad (14)$$

At this point one may notice a similarity in form between the empirical model represented by equations (3) and (4) and the a priori model represented by equations (9) and (12). Indeed, if one makes a pair-wise comparison of equation (9) with equation (3), the relationship between the empirical power factors, w and v , and the fundamental parameters of the system can be derived.

$$G_p(F_p) = F_p^w \quad \text{and} \quad G_i(F_p) = F_p^v \quad (15)$$

Clearly v is associated with MTF_i , and w is a function of the product ($\text{MTF}_p * \text{MTF}_i$). However in a well formed halftone dot $\text{MTF}_p \ll \text{MTF}_i < 1$, and the product of the two MTF functions is approximately MTF_p , and w is primarily a function of the paper MTF_p , as argued empirically in the original w, v model⁴.

Experimental Test of the Model

One dimensional halftone grey scales were generated and printed by students in the RIT School of Printing using traditional offset lithography. The halftones ranged from 0% to 100% dot (F_i from 0 to 1) and were printed at 60 LPI (2.3 cy/mm) and at 195 LPI (7.7 cy/mm) on three different papers called A, B, and C. Papers A and B were uncoated sheets similar to typical office copy paper. Paper C was a semi translucent, resin filled sheet manufactured as a tracing paper. At each value of F_i in each printed sample the printed image was examined under a microscope over a 2mm field of view. Images were captured with a Cohu model 4810 CCD camera (464 × 512 pixels) and calibrated radiometrically against a known white standard. An image histogram of reflectance factors was generated. Two peaks were observed in the histograms, one peak provided the mean ink reflectance, R_i , and the other the mean reflectance of the paper between the dots, R_p . These experimental measurements were found to vary as a function of F_i , as shown in Figures 1 and 2 for the three papers and the two halftone frequencies, $\omega_o = 2.4$ and 7.7 cy/mm. Figures 1 and 2 are displayed normalized linearly between the minimum and maximum reflectance (R_g and R_i at $F_i = 1$) observed for the different papers. This was done to facilitate comparison between different papers and print densities on the different papers. Thus the data is plotted as "Reflectance Range" rather than absolute reflectance.

The solid lines in Figures 1 and 2 are modeled from Equations (9) through (14). There are five constants in equations (9) through (14). Two of these are the reflectance of the unprinted paper, R_g , the transmittance of the ink layer, T_i . The latter can be estimated by measuring the reflectance of the ink at 100% dot, R_i , and assuming Beer's law so that $T_i = [R_i / R_p]^{1/2}$. A third constant in equations (9) through (14) is the spatial frequency of the halftones, ω_o , which is known exactly for each grey scale being modeled. The final two constants in equations (9) through (14) are used to model the two MTF

functions, MTF_p and MTF_i . In both cases we approximate the functions as $MTF = 1 / [1 + (k \omega)^2]$, so estimates of k_p for the paper MTF and k_i for the ink MTF are needed in order to model the observed data. Estimates of k_p and k_i were obtained as follows.

An estimate of k_p was made for each paper based on measured reflectance behavior. Reflectance factors over black and at infinite hiding were measured for each sheet at 550 nm with a Macbeth Color-Eye 7000. From these reflectance measurements values of the Kubelka-Munk Scattering and Absorption coefficients, K and S , were determined. From K and S , the MTF characteristic of each sheet was calculated as described by Engeldrum and Pridham^{5,6}. The result of the calculations provided an estimate of the spatial frequency, ω_p , at which each paper had an MTF value of 0.5. The corresponding characteristic distance is the inverse of this frequency, $k_p = 1 / \omega_p$. Values of $k_p = 0.263, 0.455,$ and 2.00 in units of mm were determined for papers A, B, and C respectively.

With the constants, R_p , T_i , ω_p , and k_p known, only an estimate of k_i is needed to model both R_p versus F_i and R_i versus F_i . The value of k_i is expected to be significantly less than k_p . The value of k_i used to model all of the solid lines in Figures 1 and 2 was selected to provide a good fit, as estimated by visual inspection, with the experimental data. A single value of $k_i = 0.05$ mm was chosen for all of the lines drawn to all of the data in both Figures 1 and 2.

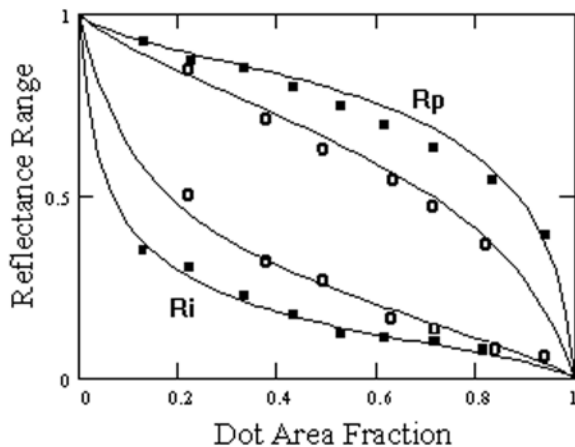


Figure 1. Reflectance Range versus F_i for Paper B printed at $w_0 = 2.4$ cy/mm (solid blocks) and at $w_0 = 7.7$ cy/mm (open circles). Both ink reflectance, R_i , and reflectance of the paper between the dots, R_p , is shown. Solid lines are modeled as described in the text.

Discussion

The grey scale of a halftone system, R versus F_i , can be modeled empirically with the Yule-Nielsen equation and three constants, R_i , R_p , n . However, the relationship between n and fundamental optical and physical metrics of the system has never been developed adequately. An alternative empirical model using factors w and v has been shown to model halftone behavior as well as the Yule-Nielsen model, but also to model the micro-reflectances, R_i and R_p versus F_i .⁴ In the work described in this report an a priori model of idealized, one dimen-

sional halftones has been developed, and the results show that the w factor is uniquely related to the scattering properties of the paper while v is related to the physical distribution of the ink.

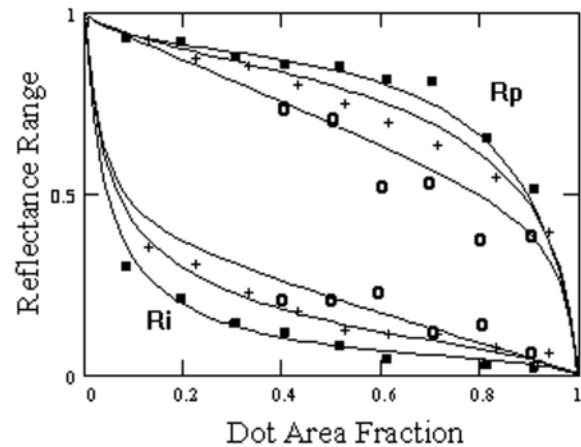


Figure 2. Reflectance Range versus F_i for Paper A, B, and C (solid block, plus, and open circles). The papers differ in their MTF constants k_p . Both ink reflectance, R_i , and reflectance of the paper between the dots, R_p , is shown. Solid lines are modeled as described in the text at 2.4 cy/mm.

The a priori model is demonstrated experimentally in Figures 1 and 2. It is particularly worth noting in Figure 1 that data for Paper B is fit well at both 60 LPI ($\omega_0 = 2.4$ cy/mm) and 195 LPI ($\omega_0 = 7.7$ cy/mm). The only parameter in the model that was changed to fit the two data sets was in fact the value of w_0 , and the values of w_0 used, 2.4 and 7.7 cy/mm, were indeed the values of the actual halftones. Similarly, the series of lines in Figure 2 were drawn using the values of k_p measured independently for the three papers. The clear advantage of such a model is the ability to predict and understand the impact of individual, independently measurable parameters of the components of the system on the tone reproduction characteristics of the system. This model is offered as an incremental advance toward that goal.

References

1. P. O. Roetling and R. P. Loce, "Digital Halftoning", *Digital Image Processing Methods*, ed. E.R. Dougherty, Marcel Dekker, Inc., NY 1994.
2. A. Murray, *J. Franklin Inst.*, **221**, 721(1936)
3. J. A. Yule and W. J. Nielsen, *Tech. Assn. Graphic Arts (TAGA) Proc.*, p65 (1951), and F. R. Clapper and J. A. Yule, *J. Opt. Soc. Am.*, **43**, 600 (1953)
4. J. S. Arney, P. G. Engeldrum, and H. Zeng, "A Modified Murray-Davies Model of Halftone Gray Scales", *TAGA*, 1995.
5. Peter G. Engeldrum, "Color Between the Dots", *J. Imag. Sci. & Tech.*, **38**, 545 (1994); see pg. 383, *this publication*.
6. Peter G. Engeldrum and Brian Pridham, "Application of Turbid Medium Theory to Paper Spread Functions Measurements", *TAGA proceedings*, 1995.

* Previously published in *IS&T's NIP11 Conference Proc.*, pp. 466-468, 1995.